

**THEORETICAL AND EXPERIMENTAL PROCEDURES IN DESIGN OF THE
PULSE-FORMING NETWORK FOR DRIVING POWER MAGNETRON VALVE**
**PROCEDIMENTOS TEÓRICO E EXPERIMENTAL NO PROJETO DE UMA LINHA
FORMADORA DE PULSOS PARA OPERAÇÃO DE UMA VÁLVULA
MAGNETRON DE POTÊNCIA**

Nivaldo Carleto*

RESUMO

Procedimentos teóricos e experimentais para projetar uma linha formadora de pulsos vêm sendo desenvolvidos para operar válvulas magnetrons de potência. O projeto teórico de uma linha formadora de pulsos é baseado na síntese teórica da rede de Guillemín. As redes obtidas neste trabalho utilizaram simulação numérica com fonte de 9kV, pulsos com largura de 0,7 μ s com frequência recorrente (PRF) de 2kHz e impedância de 31 Ω . Um aparato experimental foi construído para verificar o desempenho da PFN e os resultados obtidos são discutidos e apresentados neste trabalho.

PALAVRAS-CHAVE: Linha Formadora de Pulsos. Redes de Guillemín. Válvula Magnetron.

ABSTRACT

Theoretical and experimental procedures to design a pulse-forming network (PFN) have been developed in order to drive a high power magnetron. The theoretical pulse-forming network design approach is based on the Guillemín network synthesis theory. The networks obtained using this approach were numerically simulated to supply 9kV and 0.7 μ s pulses at 2kHz of pulse recurrence frequency (PRF) to 31 Ω impedance level. An experimental setup was assembled to verify the performance of a PFN and the obtained results of the experiment are shown and discussed in this work.

KEYWORDS: Pulse-forming Network. Guillemín Network. Valve Magnetron.

INTRODUCTION

Pulsed microwave magnetrons require the use of pulse generators that are capable of producing a train of pulses of very sharp and short duration. The most important parameters of pulse generators are pulse width, pulse power, average power, pulse recurrence frequency (PRF), duty ratio, and impedance level. The pulse generators can be also divided in two types: those in which only a small fraction of the stored electric energy is discharged into the load during a pulse, called “hard-tube pulsers”, and those in which all of the stored energy is discharged during each pulse, called “line-type pulsers”. In this last, the energy-storage device is essentially a lumped-constant transmission line. Since this component of the line-type pulser serves not only as source of the electric energy during the pulse, but also as the pulse-shaping element, it became commonly known as pulse-forming network (PFN). (GLASOE; LEBASCQZ, 1948). The PFN in a line-type pulser consists of a set of inductors and capacitors which may be put together in any one of a number of possible configurations. The configuration chosen for a particular purpose depends on the ease which the network can be fabricated, as well as, on the specific pulser characteristic desired. The theoretical basis for calculate the values of the inductance and capacitance elements of various networks are given in this paper. (GLASOE; LEBASCQZ, 1948; GUILLEMIN, 1953). In this work, it is reported some results of PFN performance that has been developed to be used in a driving magnetron circuit. The PFN features are: 31 Ω of impedance level, 2kHz of PRF, 0.7 μ s of pulse duration, and 11.4 nF of total energy-storage capacitance.

* Docente da Fatec de Taquaritinga. E-mail: nivaldo.carleto@fatectq.edu.br.

I. THEORY FUNDAMENTATION

The technique used by Guillemin's theory on design of the PFN is based on the Fourier series expansion of the desired output pulse. The trigonometric Fourier series for the rectangular pulses, suitable to drive a magnetron contains only odd terms, and it may be found by:

$$i(t) = \sum_{v=1,3,5}^{\infty} b_v \sin\left(\frac{v\pi}{\tau} t\right), \quad (1)$$

where $i(t)$ is the electric current pulse, v represent the terms odd of the series, τ is the pulse duration and b_v are the coefficients which determine the amplitude of the pulse. Each term of the Fourier series at (1) consists of a sinoidal wave at each section of the PFN, and the electric current pulse can also be written as:

$$i_v(t) = V_N \sqrt{\frac{C_v}{L_v}} \sin\left(\frac{t}{\sqrt{L_v C_v}}\right), \quad (2)$$

where, V_N , L_v , and C_v denote the PFN voltage, the inductance and the capacitance, respectively. These parameters may be determined by:

$$L_v = \frac{Z_N \tau}{4}, \quad (3)$$

and

$$C_v = \frac{4}{v^2 \pi^2} \cdot \frac{\tau}{Z_N}. \quad (4)$$

The resulting network is shown in Fig. 1, known as the type-C Guillemin network, and consists of a series of resonant LC elements connected in parallel. (GLASOE; LEBASCQZ, 1948).

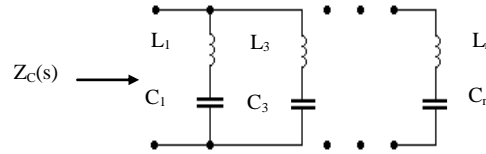


Figure 1 – PFN type-C derived by Fourier-series analysis.
Source: GUILLEMIN (1953) and GLASOE; LEBASCQZ (1948).

For a four section network type-C, the function impedance $Z_C(s)$ can be written as:

$$Z_c(s) = \frac{a_8 s^8 + a_6 s^6 + a_4 s^4 + a_2 s^2 + a_0}{b_7 s^7 + b_5 s^5 + b_3 s^3 + b_1}. \quad (5)$$

where a_i and b_j are the polynomials coefficients. The PFN type-C is inconvenient for practical use, because the inductances have appreciable distributed capacitance and capacitors have a wide range of values which makes the manufacture difficult and expensive. Therefore, it is desirable to devise equivalent networks that have different ranges of values for capacitance and inductance. For instance, using the Foster's theorem, the admittance function for network of Fig. 1 may be written, by inspection, by means of:

$$Y(s) = \sum_{v=1,3,\dots}^n \frac{C_v s}{L_v C_v s^2 + I}. \quad (6) \quad \text{or} \quad Z(s) = \frac{I}{Y(s)} = \frac{\prod_{v=1,3,\dots}^n (L_v C_v s^2 + I)}{\sum_{v=1,3,\dots}^n C_v s \prod_{\gamma=1,3,\dots}^n (L_\gamma C_\gamma s^2 + I)}. \quad (7)$$

The function $Z(s)$ may then be expanded in partial fractions about its poles, and an expression of the following form is obtained as:

$$Z(s) = \frac{A_0}{s} + \sum_{v=2,4,\dots}^{2n-2} \frac{A_v s}{B_v s^2 + I} + A_{2n} s. \quad (8)$$

For a four section network, $Z(s)$ can be written as:

$$Z_A(s) = A_0 \left[\frac{K_0}{s} + \frac{2K_2 s}{s^2 + \omega_2^2} + \frac{2K_4 s}{s^2 + \omega_4^2} + \frac{2K_6 s}{s^2 + \omega_6^2} + K_\infty s \right], \quad (9)$$

where K_n are the residues of $Z_A(s)$, ω_n are the resonance frequencies, and A_0 is a constant. Equation (9) represents the impedance function for the network of Fig. 2.

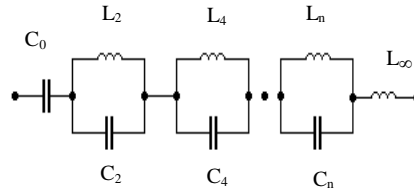


Figure 2 – PFN type-A derived by Foster's theorem.
Source: GUILLEMIN (1953) and GLASOE; LEBASCQZ (1948).

Thus, C_0 is equal to the sum of the C_v 's shown Fig. 1, and L_{2n} is equal to inductance of all the L_v 's in parallel. One additional form of physically realizable network may be found making continued-fraction expansion of the reactance or admittance functions and identifying the coefficients thus obtained with network elements. This procedure is known as Cauer's theorem and represents a ladder network (10), resulting in the type-B Guillemin network, shown in Fig. 3. This PFN correspond the transmission-line equivalent. (GLASOE; LEBASCQZ, 1948). The (10) means a series arms expressed as impedances and the shunt arms as admittances. (MUSOLINO; RAUGI; BERNARDO, 1997; KUO, 1966).

$$Z_B(s) = L'_1 s + \frac{I}{C'_2 s + \frac{I}{L'_3 s + \frac{I}{C'_4 s + \frac{I}{L'_5 s + \frac{I}{C'_6 s + \frac{I}{L'_7 s + \frac{I}{C'_8 s}}}}}}}, \quad (10)$$

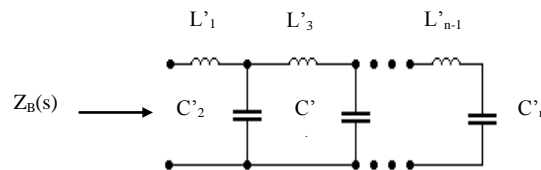


Figure 3 – PFN type-B derived by Cauer's theorem.
Source: GUILLEMIN (1953) and GLASOE; LEBASCQZ (1948).

The essential PFN obtained by canonical network forms is the type-D of the Guillemin shown in Fig. 4, which has equal capacitances. In term of the manufacture, it is desirable because the capacitors for high voltage networks are difficult item to manufacture. The negative inductances are due to compensate the modified values of the capacitances of the PFN type-C.

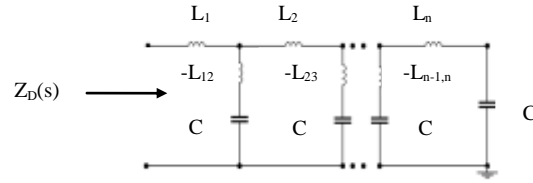


Figure 4 – PFN type-D having equal capacitances and negative inductances.
Source: GUILLEMIN (1953) and GLASOE; LEBASCQZ (1948).

The negative inductances, Fig. 4, can be realized physically by use of the mutual inductance concept (Fig. 5) known as network type-E of the Guillemin. This PFN is practical because all the inductances may be provided by single winding coil, and the capacitors may be tapped in at proper points. To find the values of inductances the PFN type-E, it is used the procedure below. (GLASOE; LEBASCQZ, 1948). For instance, for a PFN type-E of the four sections:

$$\begin{aligned} L_1 - L_{12} &= L_{E1} \\ L_2 - L_{12} - L_{23} &= L_{E2} \\ L_3 - L_{23} - L_{34} &= L_{E3} \\ L_4 - L_{34} &= L_{E4} \end{aligned} \quad (19)$$

where L_{E1} , L_{E2} , L_{E3} and L_{E4} are inductances of the type-E.

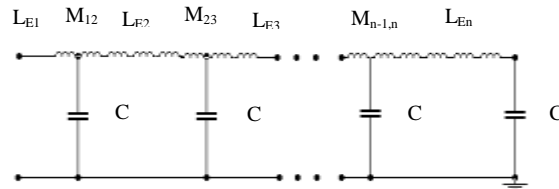


Figure 5 – PFN type-E having equal capacitances and mutual-inductances.
Source: GUILLEMIN (1953) and GLASOE; LEBASCQZ (1948).

II. MATERIALS AND METHODS

In order to investigate the characteristics of the PFN voltage-fed, a computer code to simulate the behaviour of the circuits shown in Figs. 1 to 5 was developed. The circuit analysis was carried out using the state variables approach. So, the state equations for the type-A, B, C, D and E PFNs, written using the inductor currents and the capacitor voltages as state vector elements. The system was integrated using a fourth order Runge-Kutta algorithm and the computer code was written in Turbo Pascal 1.5 programming language. (PRESS et al. 1990; CARNAHAN; LUTHER; WILKES, 1972; DESOER; KUH, 1985). The output of 0.7μs and 11.4 nF PFN was connected to a 31Ω resistive load R_L and the output pulse waveforms was obtained for a charging voltage of 9kV input. The output pulses obtained by simulation of four sections LC of PFN type-A and B with a resistive load R_L are shown in Figs. 6 and 7, respectively.

III. RESULTS AND DISCUSSION

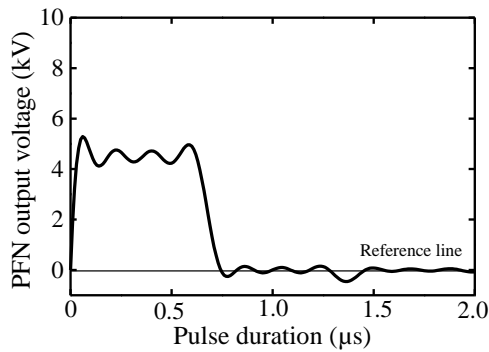


Figure 6 – Waveform pulse output of the type-A network with four-sections LC.
Source: Developed by author (2012).

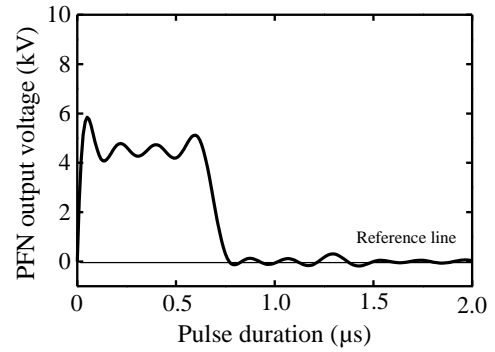


Figure 7 – Waveform pulse output of the type-B network with four-sections LC.
Source: Developed by author (2012).

The results show that networks designed to simulate a lossless transmission line have some limitations. This is evident by overshoots near of the beginning of the pulse and the oscillations during the pulse. This effect is due the first four odd terms of a rectangular pulse Fouries series in the synthesis procedure. In order to verify the accuracy of the PFN simulated, an experimental set-up shown in Fig. 8 was assembled. The output waveforms, voltage and currents pulses, in a 31Ω matched load in Fig. 9. These conditions are relevant to magnetron modulator design. The waveforms were recorded using an oscilloscope Tektronix TDS-210 connected to a computer.

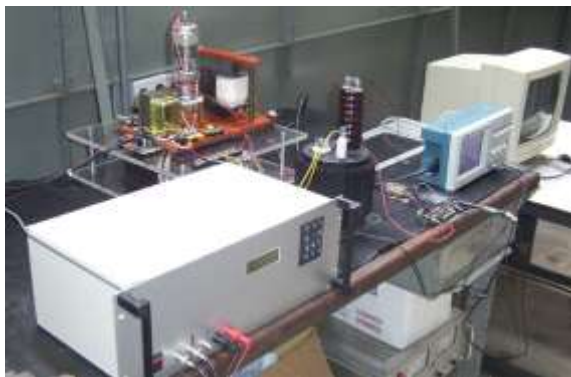


Figure 8 – Experimental assembling used for PFN performance measurements.
Source: Developed by author (2012).

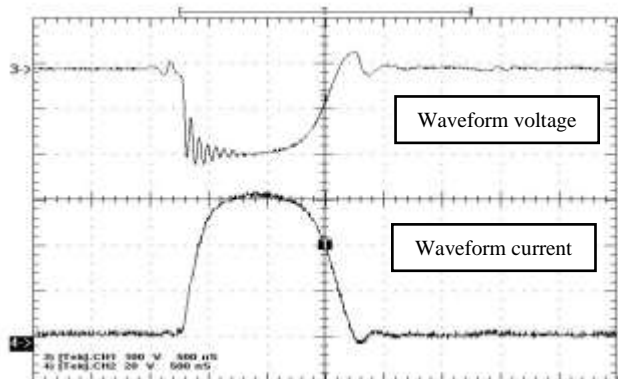


Figure 9 – The output waveforms, voltage and current pulses, in a 31Ω matched load.
Source: Developed by author (2012).

Figure 9 shows a good agreement between the theoretical and experimental results and the matching impedance can be observed between the PFN type-E and the resistive load.

CONCLUSIONS

In this work the performance of five types of PFNs were simulated and investigated. The theoretical investigation was conducted using the Guillemin synthesis network theory and the state variable approach. The resulting equation differential system was integrated using a fourth order Runge-Kutta algorithms. A test circuit modulator based on the theoretical of PFNs was assembled and the results shown that it are suitable to driving high power magnetron. The networks obtained using this approach were numerically simulated to supply 9kV and $0.7 \mu s$ pulses at 2kHz of pulse recurrence frequency (PRF) to 31Ω impedance level.

REFERENCES

- CARNAHAN, B.; LUTHER, H. A.; WILKES, J. O. **Applied numerical methods**. New York: John Wiley & Sons, Inc., 1972.
- DESOER, C. A.; KUH, E. S. **Basic circuit theory**. New York: McGraw-Hill, 1985.
- GLASOE, G. N.; LEBASCQZ, J. V. **Pulse generators**. New York: McGraw-Hill, 1948.
- GUILLEMIN, E. A. **Communication networks: the classical theory of long lines, filters and related networks**. New York: John Wiley & Sons, Inc., vol. 2, 1953.
- KUO, F. F. **Network analysis and synthesis**. New York: John Wiley, 1966.
- MUSOLINO, A.; RAUGI, M.; BERNARDO, T. Pulse-forming network optimal design for the power supply of emi launchers. **IEEE Transactions on Magnetics**. v. 33, n.1, p.480-483, 1997.
- PRESS, W. H. et al. **Numerical recipes in pascal-the art of scientific computing**. New York: Cambridge University Press, 1990.

Minicurrículo: Graduação em Engenharia Elétrica – Universidade de Marília (1996). Licenciatura Plena (Esquema-I) – Centro Paula Souza (2000). Mestrado em Ciências (Área: Tecnologia Nuclear – Materiais) – IPEN/USP/CNEN (2005). Especialização em Engenharia de Produção – UNESP (2001). Especialização em Sistemas de Informações Geográficas (Geoprocessamento) – UFSCar (2002). Especialização em Didática e Metodologia do Ensino Superior – AESA (2008). Doutorado em Educação Escolar – UNESP (2009). Docente da Faculdade de Tecnologia de Taquaritinga-SP (FATEC-TQ) e Coordenador do Grupo de Pesquisa/NDE da AESA e da Faculdade Anhanguera de Matão.

